JOURNAL OF AIRCRAFT
Vol. 50, No. 2, March–April 2013

Engineering Notes

Bang-Bang Control Applied in Airfoil Roll Control with Plasma Actuators

Qingkai Wei*
Peking University, Beijing 100871, People's Republic of China
Zhongguo Niu† and Bao Chen‡
Aviation Industry Corporation of China, Harbin 150001, People's Republic of China
and
Xun Huang§
Peking University, Beijing 100871, People's Republic of China

DOI: 10.2514/1.C031964

Nomenclature

b	=	exposed electrodes width, 1 mm
c	=	clearance distance of consecutive electrodes, 0 mm
C_z	=	aerodynamic force coefficient in z axis, $F_z/(\bar{q}S)$
C_{l_p}	=	roll moment coefficient caused by plasma actuators
d	=	chord of airfoil, 300 mm
e	=	insulated electrodes width, 4 mm
f	=	clearance distance of consecutive plasma actuators, 6 mm
F_z	=	aerodynamic force in z axis, N
(I_x, I_y, I_z)	=	the moment of inertia, $\mathrm{kg \cdot m^2}$
(I_{xy}, I_{xz}, I_{yz})	=	product of inertia, $\mathrm{kg \cdot m^2}$
L	=	total roll moment, $\mathrm{N \cdot m}$
L_p	=	plasma-induced roll moment, $\mathrm{N \cdot m}$
L_0	=	aerodynamic roll moment, $\mathrm{N \cdot m}$
O	=	coordinate origin
(p, q, r)	=	angular velocity in body axes, deg/s
$\bar{q}$	=	dynamic pressure, $1/2\rho U_\infty^2$
ρ	=	air density, $1.225\ \mathrm{kg/m^3}$
Re	=	Reynolds number based on d and U_∞
S	=	area of the measuring section, $\mathrm{mm^2}$
U_∞	=	velocity of freestream, m/s
Ws	=	wind span of airfoil, 3000 mm
α	=	angle of attack, deg
ρ	=	air density, $1.225\ \mathrm{kg/m^3}$
(ϕ, θ, ψ)	=	Euler angles, deg

Subscripts

A_T	=	target value of A

Presented as Paper 2012-4538 at the AIAA Guidance, Navigation, and Control Conference, Minneapolis, Minnesota, 13–16 August 2012; received 18 May 2012; revision received 27 September 2012; accepted for publication 27 September 2012; published online 24 January 2013.

*Ph.D. Student, Department of Aeronautics and Astronautics; weiqingkai@pku.edu.cn.

†Engineer, Aerodynamics Research Institute.

‡Senior Engineer, Aerodynamics Research Institute.

§Professor, Department of Aeronautics and Astronautics, State Key Laboratory of Turbulence and Complex Systems; huangxun@pku.edu.cn. Senior Member AIAA (Corresponding Author).

I. Introduction

PLASMA actuators, operating in atmospheric pressure air, have attracted increasing research interest in the aerospace industry over the past two decades [1,2]. Most previous publications have focused on flow-control applications that demonstrate the capability of plasma actuators and uncover, at least partially, the related fluid mechanics. In the present paper, we go one step further, studying the integration of flight control and flow control using plasma actuators, and focusing on investigating a control method suitable for plasma actuators, which constitutes the main contribution of this paper. As a demonstration, a rolling maneuver of an airfoil was controlled using only plasma actuators, which could save mechanical moving parts of ailerons. In addition, an optimal flight controller was designed and demonstrated in simulations, taking account of flow-control characteristics of plasma actuators. The proposed control method can also be considered for other flow-control applications with plasma actuators.

Various plasma actuators have been developed to address various flow-control issues, which include high-speed flow control using localized arc filament plasma actuators [3] and surface impulse discharges [4], flat-plate boundary-layer flow control by nonthermal direct current (DC) corona [5], and aerodynamic-generated noise control with glow discharges [6]. A comprehensive review of those plasma actuators can be found in the literature [2] and references therein. In this work, we adopted dielectric barrier discharge (DBD) plasma actuators [7] to control low-speed aerodynamics and, going one step further, to control flight maneuvers. A similar investigation has been conducted in a recent work [8], but using piezo-fluidic actuators. Satisfactory flight-control performance has been shown in interesting flight tests [8]. The present work differs from previous publications, focusing on the development of optimal flight-control methodology for DBD plasma actuators.

The principle of using DBD plasma actuators for flow control is not new. Figure 1a [9] shows that a DBD plasma actuator normally consists of two electrodes isolated by a dielectric material. Potential candidates for the dielectric material include silicon rubber and flame-retardant material. An alternating current (AC) power supply (Fig. 1b top) is applied to the two electrodes, between which glow discharges are generated, leading to the momentum transfer from charged nitrogen/oxygen particles to the local neutral gas through collisions. Figure 1b bottom shows the plasma potential 5 (bottom) measured in the plasma 10 mm from the exposed electrode. The collective effect is an induced fluid motion along the surface of the dielectric material, from the exposed electrode to the insulated electrode. The induced fluid motion develops vertical structures and manipulates local and global fluid mechanisms [10]. Detailed discussion of the related plasma and aerodynamic physics can be found in the literature [1].

In a previous work, deployable flow effectors were adopted on the upper surface of an NACA 0020 airfoil to delay flow separation [11]. It has been shown that the stall angle can be increased from 18 to 20 deg. In addition to aerodynamic control, one natural extension is to control airfoil flight dynamics using plasma actuators. In particular, the lift modification due to plasma can generate desired pitching and rolling moments. As a result, it is possible to save the mechanical moving parts for ailerons and flaps. However, a feedback control system has to be considered along with the plasma active flow control to achieve optimal performance. A variable-structure feedback

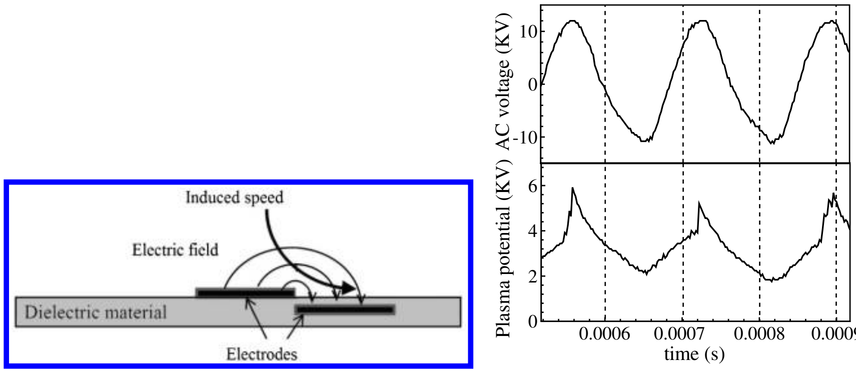

Fig. 1 The plasma actuator: a) the schematic of a DBD plasma actuator [9] and b) the AC voltage applied and the plasma potential measured.

control system has been proposed previously for cavity flow-induced noise control using glow discharges [12]. The fundamental idea behind that feedback control case was to adjust the authority of plasma actuation to a required strength, according to the feedback measurements and the variable-structure model. The modulation of plasma actuation in real time [13], however, needs complex electrical circuits and generates serious electromagnetic pollution. A simpler configuration of plasma actuators that only has two working states (on and off) was considered in this work. A bang-bang controller, also known as an on-off controller that abruptly changes actuation between upper and lower bounds, was used to feedback control the roll of an NACA 0015 airfoil. The bang-bang control method is expected to generate less electromagnetic interference and is inherently optimal in terms of its capability to achieve control objective in minimum time.

It can be seen from Fig. 1b that the AC input and the plasma potential have oscillations that suggest the "on" state of a plasma actuator changes over time. We discovered in our previous work [9] that the maximum amplitude of the plasma-induced speed rapidly varies between 6 and 8 m/s, leading to an oscillating lift force and moment. The situation will be worsened for practical cases with a time-varying power supply at various atmospheric conditions. This practical issue was considered and the disturbance rejection capability of the control method was studied in the present work. Moreover, most DBD plasma actuators have a limited control performance for high-speed flow cases. Different plasma actuators, such as impulse discharge [4] and corona [5], have been suggested for such cases. This paper focuses on low-speed aerodynamic cases (around 15 m/s) and determines applications in unmanned aerial vehicles. However, it is worthwhile to emphasize that the proposed control method is generic and could be applied to other plasma actuators.

The paper is organized as follows. Section II describes an experimental apparatus that achieves aerodynamic data for the next flight control simulation. The bang-bang control method is briefly introduced in Sec. III. A bang-bang controller is thereafter designed particularly for the airfoil roll control case with DBD plasma actuators. The integration of flight control and active flow control is simulated in Sec. IV, where the oscillations of plasma actuations and the uncertainties in aerodynamic data are considered and addressed. A brief summary is provided at the end of the paper.

II. Experimental Apparatus

Roll control of an NACA 0015 airfoil (0.3m chord, 3m span) with plasma actuators was studied in this work. Figure 2 shows the body axes used throughout the rest of the paper. The origin O of the coordinates is located at the center of gravity of the airfoil. Plasma actuators are placed on the upper surface. The span of the plasma actuators is 0.75 m, evenly covering the left and right wings. Figure 2 also shows an enlarged view of one plasma area, which is composed of 19 consecutively spaced plasma actuators. The structure and configuration of each plasma actuator are similar to those in Fig. 1a. All 19 plasma actuators are parallel circuits and can be simultaneously switched on/off to a high-voltage ac power supply. In the roll-control case, the plasma actuators on either the left or right wing can be independently switched on/off.

The aerodynamic data were obtained by conducting experiments in the FengLei-5 (FL-5) wind tunnel at the Chinese Aerodynamics Research Institute. The FL-5 low-speed wind tunnel has an open-return circuit design. The open testing section is round with a diameter of 1.5 m. The wind speed ranges from 0 to 53 m/s. Figure 3 shows the experimental setup, where the glow of plasma is clearly visible.

An NACA 0015 airfoil (0.3m chord, 0.9m span) was manufactured with Teflon and installed in the open test section. Plates that can rotate within ±24 deg are used to hold the model and test equipment as well as to maintain a good flow quality. Only the central section (0.2m span) of the model is covered with plasma actuators. As a result, the potential influence on the plasma flow control from the three-dimensional fluid and boundary flow local to the rotating plates can be omitted. The thickness of the dielectric material (epoxy polymer) is 1.5 mm. The surface of the NACA 0015 airfoil is etched to smoothly contain the plasma actuators. The electrodes are made of copper. The width of the exposed copper electrodes is $b = 1$ mm. The width of the insulated electrodes is $e = 4$ mm. The clearance distance c between two electrodes is zero. The clearance distance between two plasma actuators is $f = 6$ mm. It should be pointed out that the previous values are empirically chosen, reflecting a tradeoff between the experimental geometry limitation and plasma performance. It can be seen that the simulation setup shares the

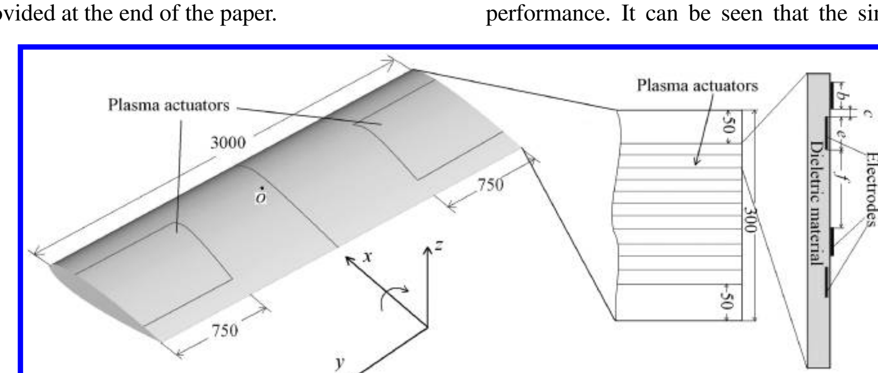

Fig. 2 The schematic of the NACA 0015 airfoil and the layout of plasma actuators for the roll-control simulation case (dimensions are in millimeters).

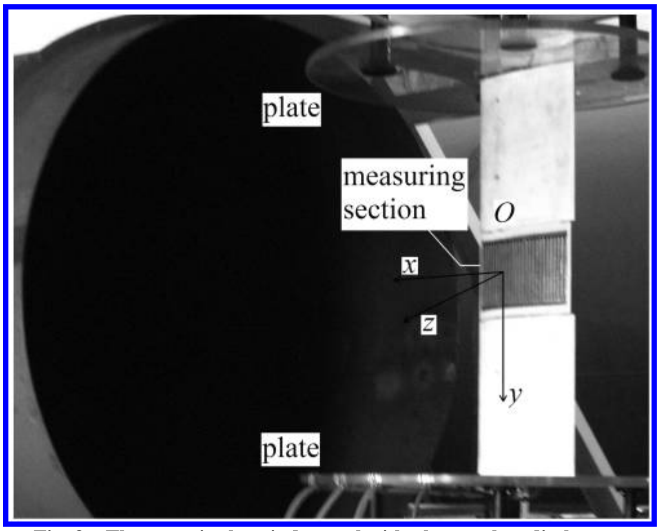

Fig. 3 The setup in the wind tunnel with plasma glow discharges.

same geometrical setup as plasma actuators. Hence, the plasma-induced roll momentum can be derived from the aerodynamic force measurement, although the experimental model is just part of the simulation model in Fig. 2, which is for convenience in experiment. The force and moment coefficients of the simulation model, with and without plasma actuation, were respectively calculated based on experimental results, taking geometry differences into account. The AC voltage applied was 22 kV and 180 W at 4.7 kHz. The following simulation in Sec. IV adopt experimental results here achieved at $U_\infty = 15$ m/s, where U_∞ is the freestream velocity. The corresponding Reynolds number with respect to the chord length is approximately 3×10^5.

The experimental measurements of aerodynamic force are shown in Fig. 4a. The force coefficient $C_z = F_z/(\bar{q}S)$, where F_z is the force along the z axis, S is the area of the airfoil, $\bar{q}$ is dynamic pressure $(\rho U_\infty^2/2)$, and ρ is the air density. It can be seen that the amplitude of C_z increases almost linearly along with the increase of α. The slope does not match the thin airfoil theory possibly because the application of DBD plasma actuators causes small changes in the geometry of the measured airfoil model. Considering that this result came from the wind tunnel experiment, the following work is still based upon it. The C_z quickly drops beyond the so-called stall angle (C_z is not the traditional lift coefficient). Plasma actuation can slightly increase the stall angle by almost 2 deg, whereas the angle of attack is approximately 20 deg. On the other hand, the increase in C_z due to plasma actuation at low angles of attack is quite small. For example, we can only have a 3.56% increase (from 0.705 to 0.73) in $|C_z|$ at $\alpha = 12$ deg. Figure 4b shows the plasma-induced roll moment coefficient that is used in the simulations, where plasma actuators in the left airfoil are activated and the right ones are deactivated. The relatively large roll moment around 20 deg is caused by the increased the stall angle using plasma actuation. The roll moments at other angles are small. However, it can be seen in the following simulations that even such small roll moments can achieve acceptable roll control performance.

III. Bang-Bang Controller Design

In control theory, bang-bang control is well known as the minimum-time optimal-feedback control method, whose control inputs are constrained to only two levels [14]. The roll dynamics of the airfoil can be described for the airfoil roll control case by

$$L = I_x\dot{p} - (I_y - I_z)qr + I_{xy}(pr - \dot{q}) - I_{xz}(pq + \dot{r}) + I_{yz}(r^2 - q^2)$$
$$L = L_0 + L_p$$
$$p = \dot{\phi} - (\sin\theta)\dot{\psi} \tag{1}$$

where (I_x, I_y, I_z) is the moment of inertia in body axes, I_{xy} is the product of inertia about the ox and oy axes, I_{xz} is the product of inertia about the ox and oz axes, and I_{yz} is the product of inertia about the oy and oz axes. The angular velocities are represented by (p, q, r). The Euler angles of the airfoil with respect to a flat earth are (ϕ, θ, ψ) L is the total roll moment, which consists of aerodynamic roll moment L_0 and plasma-induced roll moment L_p.

The moment of inertia $I_{xy} = I_{yz} = 0$, as the airfoil is symmetric about the oxz plane and the airfoil has a uniform mass distribution. In addition, the pitch and yaw motions are excluded for simplicity, i.e., $q \equiv 0$, $r \equiv 0$, $\psi \equiv 0$, and $\theta \equiv 0$. As a result, $\dot{\phi} = p$, where p is the roll angular velocity in body axes.

It is implicitly assumed that the airfoil is already trimmed without plasma actuation. The plasma-induced moment is $L_p = M$ in case the plasma actuators on the left wing are activated. Similarly, $L_p = -M$ if the plasma actuators on the right wing are activated. The scenario in which all plasma actuators on both wings are activated was not considered in this work. In summary, the roll dynamics can be simplified to

$$\ddot{\phi} = \pm M/I_x \tag{2}$$

which is a simple model, because this work primarily focuses on the attempt of control method investigation for plasma actuators applied in flight control. This method can also be applied to more accurate physical models. A state space model can be accordingly formulated as

$$\begin{bmatrix} \dot{\phi} \\ \ddot{\phi} \end{bmatrix} = \begin{bmatrix} 0 & 1 \\ 0 & 0 \end{bmatrix}\begin{bmatrix} \phi \\ \dot{\phi} \end{bmatrix} + \begin{bmatrix} 0 \\ M/I_x \end{bmatrix}u, u = \pm 1 \tag{3}$$

where the control input u is the sign of plasma-induced roll moment.

With no loss of generality, the initial state of the airfoil is assumed at $[\phi(0), \dot{\phi}(0)] = [0, 0]$. The objective of the roll control is

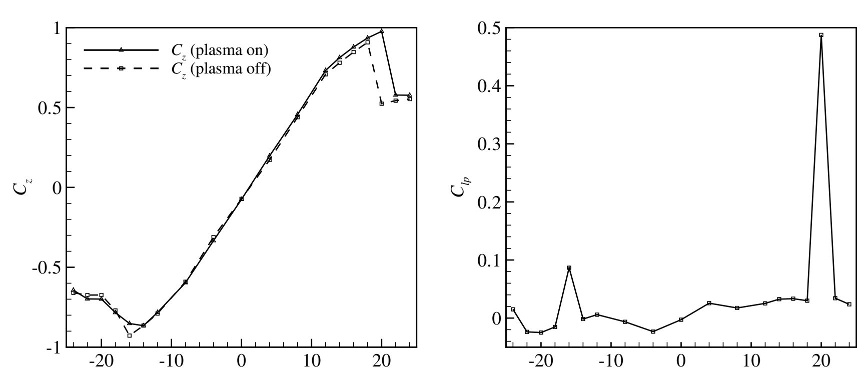

a) b)

Fig. 4 a) Experimental results of C_z at $U_\infty = 15$ m/s, where the corresponding Reynolds number is 3×10^5; and b) the related plasma-induced roll moment coefficient in the simulations.

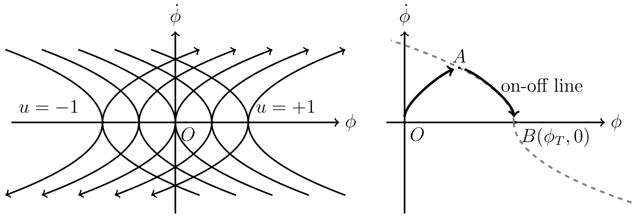

a) b)

Fig. 5 Schematics of bang-bang control: a) phase line with $u = \pm 1$; b) the on–off line for roll control.

$[\phi(t), \dot{\phi}(t)] = [\phi_T, 0]$, where ϕ_T is the target roll angle. It is straightforward to achieve

$$\begin{cases} \dot{\phi} = \frac{M}{I_x} t \\ \phi = \frac{M}{2I_x} t^2 + C_1 \end{cases} \quad \text{for u} = 1;$$

$$\begin{cases} \dot{\phi} = -\frac{M}{I_x} t \\ \phi = -\frac{M}{2I_x} t^2 + C_1 \end{cases} \quad \text{for u} = -1 \tag{4}$$

where C_1 is a constant value. Figure 5a shows the phase line $\phi = \pm \frac{1}{2M/I_x} (\dot{\phi})^2 + C_1 (u = \pm 1)$, which is achieved by eliminating the variable t in Eq. (4).

As shown in Fig. 5b, the initial state $[\phi(0), \dot{\phi}(0)] = [0, 0]$ is at point O. The control objective $[\phi(t), \dot{\phi}(t)] = [\phi_T, 0]$ is at B. As a result, the initial control input should be set to $u = +1$ to turn the initial state O along the phase line $\phi = \frac{1}{2M/I_x} \dot{\phi}^2$ to state A, which is on the intersection on the other phase line $\phi = -\frac{1}{2M/I_x} \dot{\phi}^2 + \phi_T (\dot{\phi} > 0)$. The control input switches to $u = -1$ once A is reached. The state thereafter advances to the target state B $[\phi_T, 0]$.

A so-called on–off line (the dashed line in Fig. 5b) depends on ϕ_T and can be formulated as

$$\phi = -\frac{1}{2M/I_x} \dot{\phi} |\dot{\phi}| + \phi_T \tag{5}$$

In summary, for any initial solution, the desired control input u is

$$u = \begin{cases} +1; & \left(\phi + \frac{1}{2M/I_x} \dot{\phi}|\dot{\phi}| - \phi_T < 0\right) \quad \text{or} \quad \left(\phi + \frac{1}{2M/I_x} \dot{\phi}|\dot{\phi}| - \phi_T = 0, \dot{\phi} < 0\right) \\ -1; & \left(\phi + \frac{1}{2M/I_x} \dot{\phi}|\dot{\phi}| - \phi_T > 0\right) \quad \text{or} \quad \left(\phi + \frac{1}{2M/I_x} \dot{\phi}|\dot{\phi}| - \phi_T = 0, \dot{\phi} > 0\right) \end{cases} \tag{6}$$

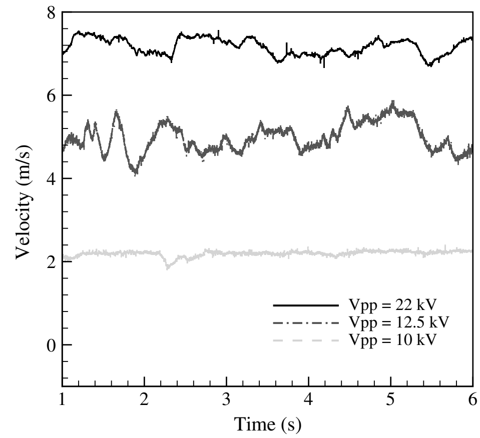

Fig. 8 Measurements of plasma-induced velocities in the stationary atmospheric pressure air.

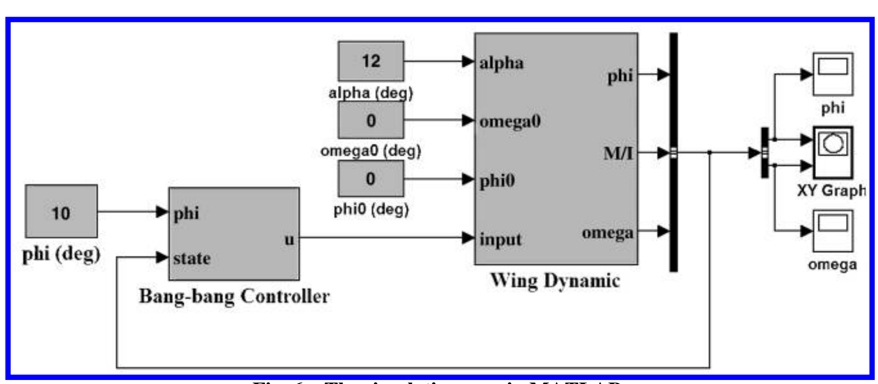

Fig. 6 The simulation case in MATLAB.

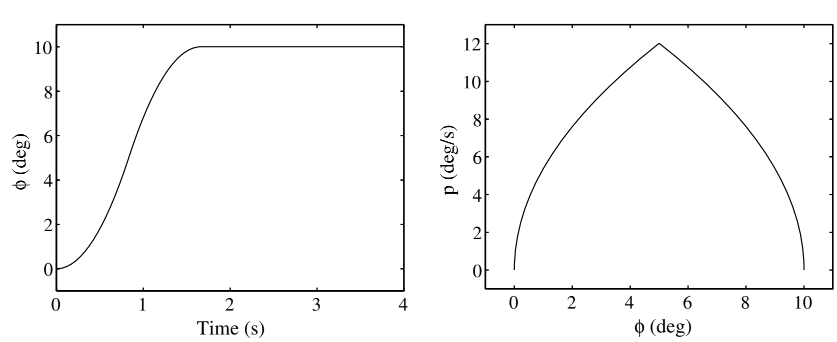

a) b)

Fig. 7 Dynamics during the airfoil roll from 0 to 10 deg at $\alpha = 12$ deg and $U_\infty = 15$ m/s: a) roll angle dynamics and b) phase line.

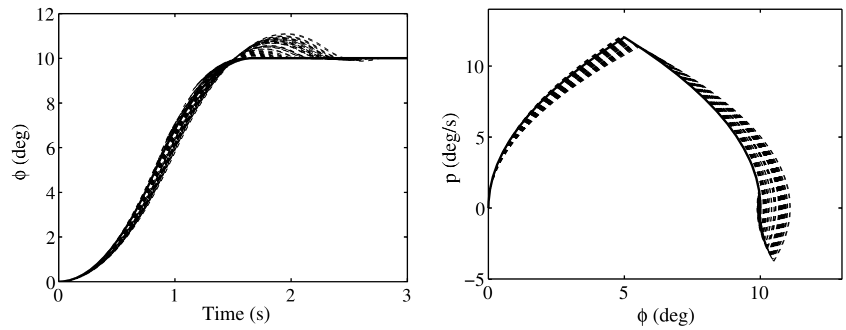

a) b)

Fig. 9 Monte Carlo simulation results of roll control from 0 to 10 deg, where the plasma-induced roll momentum is randomly chosen: a) roll angle dynamics and b) phase line.

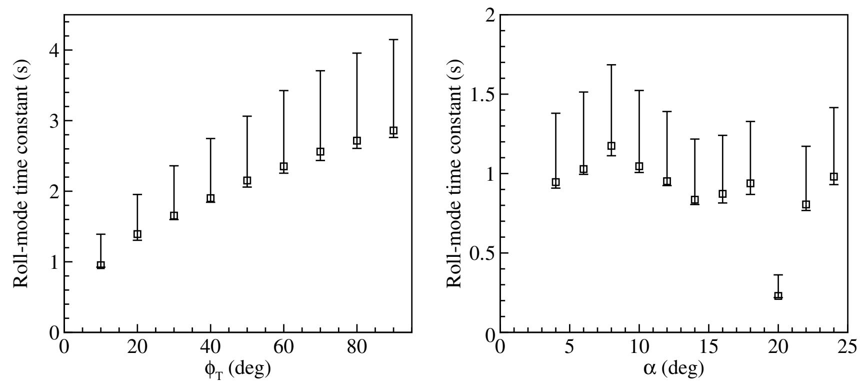

a) b)

Fig. 10 Roll-mode time constant error bar: a) $\alpha = 12$ deg and b) $\phi = 10$ deg.

IV. Simulation and Discussion

Numerical simulations were conducted to demonstrate airfoil roll control using plasma actuators. Figure 6 shows the implementation of the simulation case in MATLAB. The block labeled bang-bang controller implements Eq. (6). The wing dynamic block implements the airfoil roll dynamics. The moment of inertia I_x is 4.05 $\mathrm{kg \cdot m^2}$, given the span length (3 m) and the uniformly distributed mass (5.4 kg) with a density of 200 $\mathrm{kg/m^3}$. The dynamic pressure is 137.8 Pa, given the air density of 1.225 $\mathrm{kg/m^3}$ and mean flow velocity of 15 m/s.

Figure 7 shows the simulation results for $\phi_T = 10$ deg, where the angle of attack $\alpha = 12$ deg, at which it is implicitly assumed that the airfoil is already trimmed. It can be seen that plasma-induced moments roll the airfoil to the target angle in approximately 1.5 s.

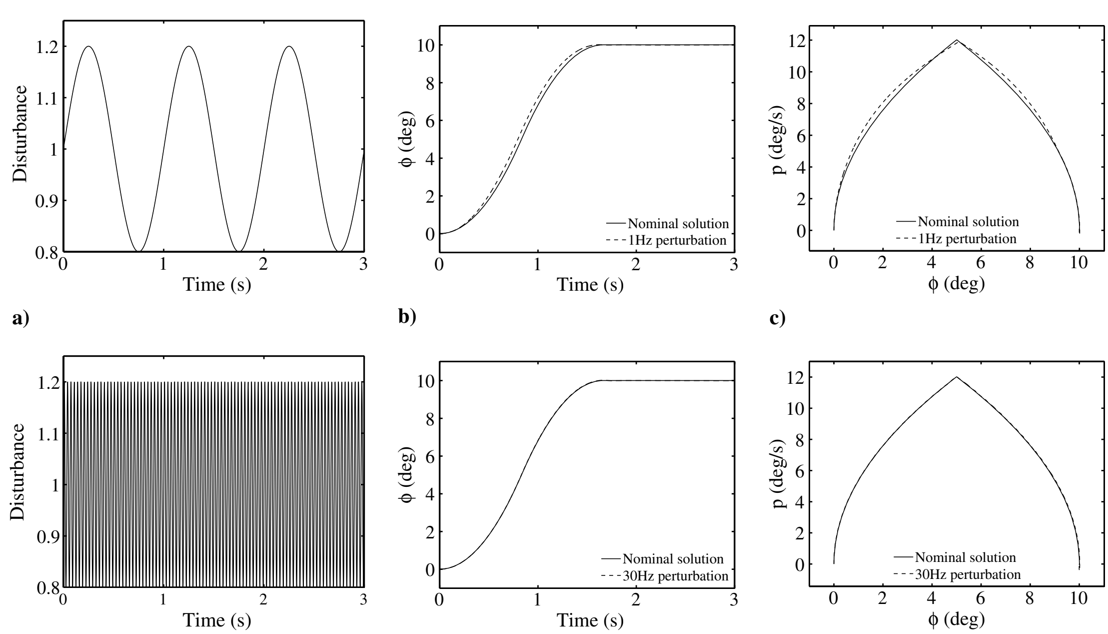

a) b) c)

d) e) f)

Fig. 11 Simulation results with a, d) 20% variance of plasma-induced roll moments at 1 and 30 Hz, b, e) corresponding roll angle dynamics, and c, f) related phase lines.

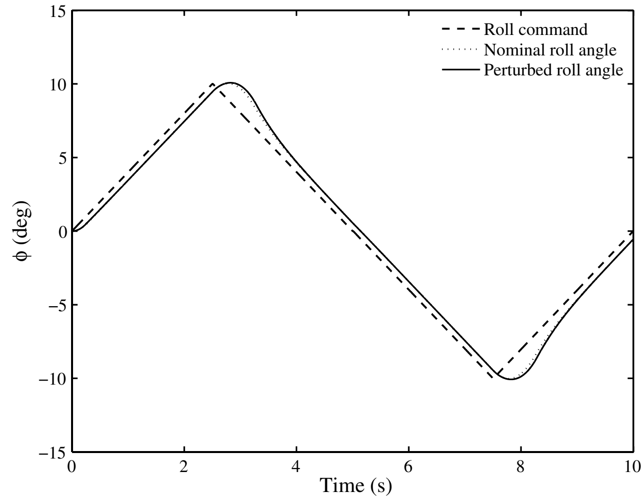

Fig. 12 Roll angle dynamics for a series of roll commands.

Almost no overshoot can be found. Figure 8 is the plasma-induced velocity measured at 20 mm downstream from the exposed electrodes [10]. It can be seen that the plasma-induced velocities oscillate at a high-voltage input ($Vpp = 22$ and 12.5 kV). The variance is approximately 20%.

A Monte Carlo simulation was conducted to examine the effect of the varying plasma actuations on the roll control. The plasma-induced momentum is approximated with $\pm 20\%$ uncertainty about the nominal values C_{l_p} in Fig. 4b. Figures 9 and 10 show the Monte Carlo simulation results. The roll moment coefficient is randomly chosen between $0.8C_{l_p}$ and $1.2C_{l_p}$ in 100 repeated simulations. It can be seen in Fig. 9 that overshoots could appear for varied plasma-induced momentums. The phase line slightly changes as well. In addition, the rise time of the control has been affected.

Figure 10 quantitatively shows the changes, where the square symbols denote nominal outcomes and error bars represent possible time constant ranges calculated by the Monte Carlo simulation if aerodynamic coefficients are varied by $\pm 20\%$. The roll-mode time constants (the time needed to reach 63.2% of the target roll angle) for different roll targets (from 10 to 90 deg) at $\alpha = 12$ deg are shown in Fig. 10a. According to the MIL-F-8785C specification of flying qualities, the maximum roll-mode time constant is 10 s for level 3 flights of light airplanes. Figure 10 shows that this flying qualities section can be satisfied with the proposed bang-bang controller and plasma actuators. Figure 10b shows the roll-mode time constants for 10 deg at various angles of attack between 4 and 24 deg. It can be seen that the roll control is most effective at a high angle of attack around 20 deg, where the flow separation has been delayed with plasma actuation. The flying qualities (<10 s) are still satisfied.

It is more practical to regard the almost 20% aerodynamic variance as an instantaneous disturbance to the controlled system. The Fourier spectrum of the results in Fig. 8 largely lies between 1 and 30 Hz. As a result, the plasma-induced roll moments are varied at these two frequencies (Figs. 11a and 11d) to verify the robustness of the proposed control method still with the case of roll control from 0 to 10 deg at $\alpha = 12$ deg. Figures 11b and 11c show that a slight change can be found in the roll dynamics and phase line (<5%) for the 1-Hz perturbation case. Figures 11e and 11f suggest the control method is insensitive to the relatively high frequency disturbance at 30 Hz. Almost no change can be found in the roll dynamics and phase line. As a result, the proposed bang-bang control is robust and can address practical issues of plasma actuators.

Finally, Fig. 12 shows the roll dynamics of the airfoil commanded by a series of roll commands. The nominal roll angles with constant plasma-induced roll moments satisfactorily track the roll commands with a less than 0.5-s time delay. On the other hand, the perturbed roll angles with 20% variance of moments at 1 Hz also follow the roll commands well, suggesting the good performance of the proposed control method.

The previous simulations are operated under a constant angle of attack, when the plasma-induced roll moment is a constant number. To estimate the real condition, the change in angle of attack α is considered in the following simulation. Figure 13 shows the roll control effect when the model rolls from 0 to 10 deg when α is time-variable, as Fig. 13a shows. The angle of attack α is chosen when the plasma-induced roll moment is positive, not only at the stall angle. Simulation results show the roll control is realizable, although the

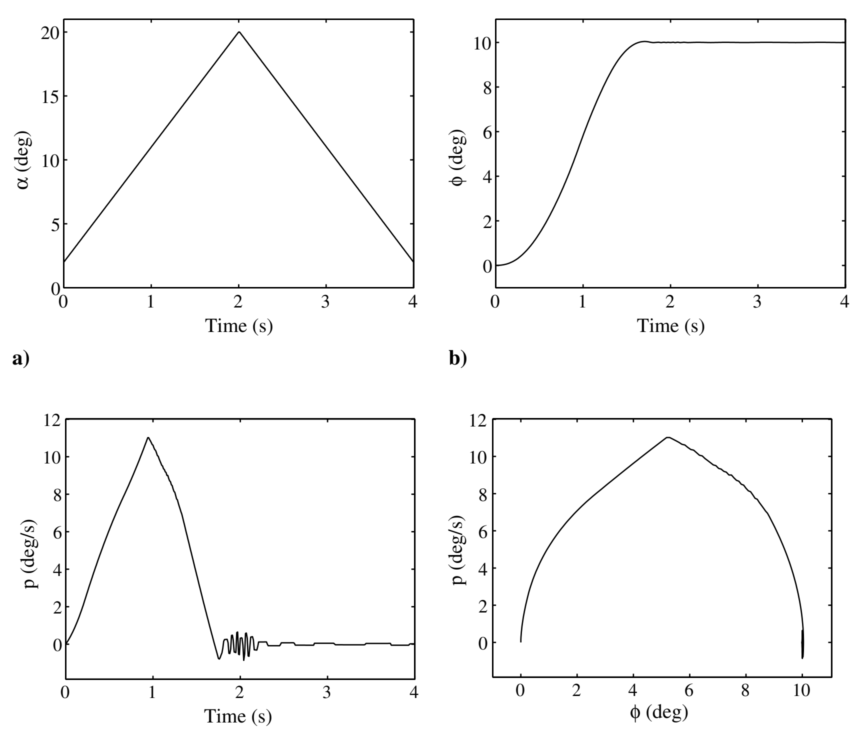

Fig. 13 Simulation results when α is changing: a) change in α over time, b) roll angle dynamics, c) roll angle velocity dynamics, and d) phase line.

phase line in Fig. 13d is little different from that of previous cases. Based on this result, more complicated flight control can adopt plasma actuators to reduce mechanical parts.

V. Conclusions

The main contribution of this article is to integrate flight control with active flow control using plasma actuators by investigating a control method specifically for plasma actuators in flight control. The bang-bang control method has been proposed for plasma actuators, taking account of practical issues such as limited actuation states with instantaneously varied aerodynamic control performance. Flow-control effects have been examined in wind tunnel experiments, which show that the plasma authority for flow control is limited. Flow-control effects are only obvious at pitch angles near the stall. However, flight-control simulations suggest that, using the proposed optimal control method, even those small plasma-induced roll moments can satisfactorily fulfill the maneuver tasks and meet flight quality specifications. In addition, the disturbance from volatile plasma-induced roll moments can be adequately rejected. Hence, the proposed bang-bang control method is a promising candidate of control design methodology for plasma actuators. Ongoing and future work includes airfoil flight control in wind tunnel and final flight tests.

Acknowledgments

This work has been partially supported by the National Science Foundation Grant of China (90916003) and the Science Foundation of Aeronautics of China (20090771001 and 20101271004).

References

[1] Roth, J., Sherman, D., and Wilkinson, S., "Electrohydrodynamic Flow Control with a Glow-Discharge Surface Plasma," *AIAA Journal*, Vol. 38, No. 7, 2000, pp. 1166–1172.
doi:10.2514/2.1110

[2] Mosreau, E., "Airflow Control by Non-Thermal Plasma Actuators," *Journal of Physics D: Applied Physics*, Vol. 40, No. 3, 2007, pp. 605–636.
doi:10.1088/0022-3727/40/3/S01

[3] Kim, J., Kastner, J., and Samimy, M., "Active Control of a High Reynolds Number Mach-0.9 Axisymmetric Jet," *AIAA Journal*, Vol. 47, No. 1, 2009, pp. 116–128.
doi:10.2514/1.36801

[4] Gnemmi, P., Charon, R., Dupéroux, J., and George, A., "Feasibility Study for Steering a Supersonic Projectile by a Plasma Actuator," *AIAA Journal*, Vol. 46, No. 6, 2008, pp. 1308–1317.
doi:10.2514/1.24696

[5] Moreau, E., Léger, L., and Touchard, G., "Effect of a DC Surface-Corona Discharge on a Flat Plate Boundary Layer for Air Flow Velocity up to 25 m/s," *Journal of Electrostatics*, Vol. 64, No. 3–4, 2006, pp. 215–225.
doi:10.1016/j.elstat.2005.05.009

[6] Huang, X., and Zhang, X., "Plasma Actuators for Noise Control," *International Journal of Aeroacoustics*, Vol. 9, No. 4, 2010, pp. 679–704.
doi:10.1260/1475-472X.9.4-5.679

[7] Enloe, C., McLaughlin, T., VanDyken, R., Kachner, K., Jumper, E., and Corke, T., "Mechanisms and Responses of a Single Dielectric Barrier Plasma Actuator: Plasma Morphology," *AIAA Journal*, Vol. 42, No. 3, 2004, pp. 589–594.
doi:10.2514/1.2305

[8] Seifert, A., David, S., Fono, I., Stalnov, O., and Dayan, I., "Roll Control via Active Flow Control: From Concept to Flight," *Journal of Aircraft*, Vol. 47, No. 3, 2010, pp. 864–874.
doi:10.2514/1.45910

[9] Huang, X., Zhang, X., and Li, Y., "Broadband Flow-Induced Sound Control Using Plasma Actuators," *Journal of Sound and Vibration*, Vol. 329, No. 13, 2010, pp. 2477–2489.
doi:10.1016/j.jsv.2010.01.018

[10] Huang, X., and Zhang, X., "Streamwise and Spanwise Plasma Actuators for Flow-Induced Cavity Noise Control," *Physics of Fluids*, Vol. 20, No. 3, 2008, pp. 037101-1–037101-10.
doi:10.1063/1.2890448

[11] Patel, M., Tilmann, C., and Ng, T., "Active Transparent Stall Control System for Air Vehicles," *Journal of Aircraft*, Vol. 40, No. 5, 2003, pp. 993–997.
doi:10.2514/2.6885

[12] Huang, X., Chan, S., Zhang, X., and Gabriel, S., "Variable Structure Model for Flow-Induced Tonal Noise Control with Plasma Actuators," *AIAA Journal*, Vol. 46, No. 1, 2008, pp. 241–250.
doi:10.2514/1.30852

[13] Huang, X., Chan, S., and Zhang, X., "Atmospheric Plasma Actuators for Aeroacoustic Applications," *IEEE Transactions of Plasma Science*, Vol. 35, No. 3, 2007, pp. 693–695.
doi:10.1109/TPS.2007.89678

[14] Lewis, F., and Syrmos, V., *Optimal Control*, Wiley-Interscience, New York, 1995, pp. 284–297.